DOI:
10.1152/ajpendo.00042.2017

Document Version
Peer reviewed version

Glycemic control after metabolic surgery: a Granger causality and graph analysis

[1]Elena Previti, [1]Serenella Salinari, [2]Alessandro Bertuzzi, [3]Esmeralda Capristo,

[4, 5] Stephan Bornstein, [3, 5]Geltrude Mingrone

[1]Department of Computer, Control, and Management Engineering "Antonio Ruberti," University of Rome "Sapienza," Rome, Italy

[2]CNR-Institute of Systems Analysis and Computer Science (IASI), Rome, Italy

[3]Department of Internal Medicine, Catholic University, Rome, Italy

[4]Department of Medicine III, Universitätsklinikum Carl Gustav Carus an der Technischen Universität Dresden, Dresden, Germany

[5]Diabetes and Nutritional Sciences, Hodgkin Building, Guy's Campus, King's College London, London, United Kingdom

Corresponding author

Geltrude Mingrone, MD, PhD

Department of Internal Medicine

Catholic University

Largo A. Gemelli 8 – 00168 Rome, Italy

Email: gmingrone@rm.unicatt.it; geltrude.mingrone@kcl.ac.uk

Word count: 4094

2 Tables and 2 figures

ABSTRACT

To examine the contribution of Non-Esterified Fatty-Acids (NEFA) and incretin to insulin-resistance and diabetes amelioration after malabsorptive metabolic-surgery that induces steatorrhea. In fact, NEFA infusion reduces glucose-stimulated insulin secretion and high-fat diets predict diabetes development. Six healthy-controls, 11 obese and 10 Type-2-Diabetic (T2D) subjects were studied before and 1 month after Bilio-Pancreatic Diversion (BPD). Twenty-four hours plasma glucose, NEFA, insulin, C-peptide, glucagon-like peptide-1 (GLP1) and gastric-inhibitory-polypeptide (GIP) time courses were obtained and analyzed by Granger causality and graph analyses. Insulin sensitivity and secretion were computed by the oral glucose minimal-model. Before metabolic-surgery NEFA had the strongest influence on the other variables in both obese and T2D subjects. After surgery, GLP1 and C-peptide controlled the system in obese and T2D subjects. Twenty-four hours GIP levels were markedly reduced after BPD. Finally, GLP1 played a central role, but also insulin and C-peptide had a comparable relevance in the network of healthy controls. After BPD insulin sensitivity was completely normalized in both obese and T2D individuals. Increased 24-hours GLP1 circulating levels positively influence glucose homeostasis in both obese and T2D subjects who underwent a malabsorptive bariatric operation. In these latter, the reduction of plasma GIP also contributed to the improvement of glucose metabolism. It is possible that the combination of a pharmaceutical treatment reducing GIP and increasing GLP1 plasma levels will contribute to a better glycemic control in T2D. The application of Granger causality and graph-analyses shed new light on the patho-physiology of metabolic surgery.

INTRODUCTION

Obesity and type 2 diabetes (T2D) are strictly associated. At least 285 million people worldwide are affected by diabetes and this number is expected to raise to 438 million by 2030 (21). In the United States, more than 1 in 3 adults are obese and 1 in 20 adults are morbidly obese (34).

Together with a reduced physical activity, an excessive caloric intake represents a major driver of the global epidemics of obesity and type 2 diabetes. A large body of literature has shown that in experimental animals a high fat diet, particularly if rich in saturated fat, determines insulin resistance. Assessing the association between diet and T2D development over a 12-year time frame, van Dam et al. (50) found that consumption of a high fat diet and high intake of saturated fat are associated with the risk of increased diabetes. However, this significance disappeared when adjusting for the Body Mass Index (BMI), meaning that obesity was a stronger predictor of T2D. Prolonged non-esterified fatty acids (NEFA) infusion reduces glucose-stimulated insulin secretion and the disposition index (28). In addition, a raise in plasma NEFA leads to reduced insulin clearance (6, 7).

Although lifestyle modifications successfully reduce the incidence of diabetes in high risk populations (49, 25), the compliance in the long term is poor (18). Metabolic surgery is an effective approach for the treatment of both obesity and T2D (12, 41, 31). However, its mechanism of action remains to be elucidated. In fact, the rapid resolution of diabetes and insulin resistance before any significant change in body weight challenge the weight loss as the only mechanistic effect (47, 36, 17).

Bilio-pancreatic diversion (BPD) is a type of metabolic operation associated with a massive lipid malabsorption and, consequently, with a dramatic circulating lipid lowering (30) and diabetes remission (31). It is, therefore, possible that the daily reduction of NEFA can be associated with the lowering of glucose circulating levels; alternatively 24 hour changes in glucagon-like peptide 1

(GLP1) and/or gastric inhibitory polypeptide (GIP) might drive the improvement of glucose control following BPD.

In this study, we apply for the first time the Graph theory approach associated with Granger causality test to time series of metabolites and hormones in order to assess the interactions among hormones (insulin, C-peptide, GLP1 and GIP) and energy substrates, such as glucose and NEFA, as well as their directions.

MATERIALS AND METHODS

We studied 11 obese subjects (4 women and 7 men, age 42.8 ± 2.6 y) with normal glucose tolerance, 10 obese subjects with type-2 diabetes (2 women and 8 men, 43.2 ± 2.4 y) and 6 healthy controls (4 women and 2 men, 43.1 ± 2.3 y). The anthropometric characteristic of the subjects are reported in Table 1. The study protocol was approved by the Ethical Committee of the Catholic University of Rome. All participants provided written informed consent to participate in the study. Additional written informed consent was obtained prior to the surgical procedures.

Bilio-Pancreatic Diversion

BPD (42, 29) consists of a ~60% distal gastric resection with stapled closure of the duodenal stump. The residual volume of the stomach is ~300 ml. The small bowel is transected at 2.5 m from the ileo-cecal valve, and its distal end is anastomosed to the remaining stomach. The proximal end of the ileum, comprising the remaining small bowel carrying the bilio-pancreatic juice and excluded from food transit, is anastomosed in an end-to-side fashion to the bowel 50 cm proximal to the ileo-cecal valve. Consequently, the total length of absorbing bowel is brought to 250 cm, the final 50 cm of which, the so-called common channel, represents the site where ingested food and bilio-pancreatic juices mix.

Body composition

Total body composition was determined by dual-energy x-ray absorptiometry using a Lunar Prodigy whole-body scanner (GE Medical Systems, Madison, WI). The subjects were scanned in light clothing lying flat on their backs and with arms by their side. Fat mass (FM) and fat free mass (FFM) were obtained in kg.

Twenty-four–hour studies

All participants underwent the metabolic study at baseline and at 1 month after BPD, spending 24 h (starting at 08:00 hours) on a metabolic ward. During this period, 4 meals were administered.

The patients received a total daily energy intake of 30 kcal (16.9% of energy as protein, 34.6% fat and 48.5% carbohydrates) per kg_{FFM} distributed as 14% at breakfast (09:00 hours), 36% at lunch (12:00–13:00 hours), 16% as an afternoon snack (16:00–16:30 hours) and 34% at dinner (19:00–20:00 hours). The food given and returned was weighed to the nearest gram on precision scales (KS-01; Rowenta, Berlin, Germany). Blood samples were drawn every 60 min from a central venous catheter for the measurement of glucose, NEFA, insulin, C-peptide, GLP1 and GIP concentrations.

Analytical methods

Plasma samples were immediately centrifuged and stored at −80°C before analyses. Plasma glucose was measured by the glucose oxidase method (Beckman, Fullerton, CA). Plasma insulin was assayed by microparticle enzyme immunoassay (Abbott, Pasadena, CA) with a sensitivity of 1 μU/mL and an intra-assay CV of 6.6%. C-peptide was assayed by RIA (MYRIA; Technogenetics, Milan, Italy) as follows: a minimal detectable concentration, 17 pmol/L, and inter- and intra-assay CVs of 3.3–5.7% and 4.6 –5.3%, respectively.

NEFA levels were determined using a colorimetric assay (HR Series NEFA-HR; Wako Diagnostics, Richmond, VA). For incretin analysis, venous blood was collected in ice-chilled EDTA dipotassium–treated tubes containing aprotinin (500 kallikrein inhibitory units per milliliter of blood), and then stored at −80°C. Immunoreactive GIP levels were determined using 0.1 mL plasma in a human GIP RIA kit (Peninsula Laboratories, Belmont, California). Intra-assay CV was 6% and interassay CV was 8 and 12% for 20 and 80 pmol/L standards, respectively. Total GLP1 was measured by RIA (Linco Research); intraassay and interassay CVs were 9–14% and 11–20%,

respectively. This assay has 100% specificity for GLP1 (7–36), GLP1 (9 –36), and GLP1 (7–37) and does not cross-react with glucagon (0.2%), GLP2 (<0.01%), or exendin (<0.01%).

Mathematical Models

Granger causality

Wiener–Granger causality ("G-causality") is a statistical notion of causality (16) applicable to time series data, based on predictability and precedence. A variable Y that evolves over time is said to G-cause another evolving variable X if the past of Y contains information that helps to predict the future of X over and above the information already contained in the past of X. In this predictive interpretation the G-causality between two variables, Y and X, may be written as $F_{Y\rightarrow X}$, which represents quantitatively the "degree to which the past of Y helps predict X, over and above the degree to which X is already predicted by its own past" (2).

The X component at time t, X_t, is assumed to depend on the past of Y according to the equation (autoregressive model):

$$X_t = \sum_{k=1}^{p} A_{xx,k} \cdot X_{t-k} + \sum_{k=1}^{p} A_{xy,k} \cdot Y_{t-k} + \varepsilon_{x,t} \ , \qquad (1)$$

where X and Y are, in general, random vectors, $A_{xx,k}$ and $A_{xy,k}$ are matrices, ε is a noise term (regression residuals), and p is the model order. In particular, there is no conditional dependence of X on the past of Y (reduced regression) if

$$A_{xy,1} = A_{xy,2} = \cdot \cdot \cdot = A_{xy,p} = 0.$$

Therefore, technically, the G-causality is a test statistic for the null hypothesis of zero causality:

$$H_0: A_{xy,1} = A_{xy,2} = \cdot \ \cdot \ \cdot = A_{xy,p} = 0, \qquad (2)$$

and the null hypothesis will be rejected if the inclusion of the Y-term in Eq. (1) substantially improves the fitting capacity of the model.

In the presence of multivariate processes with variables X, Y and Z, where Z is an exogenous variable that affects X and Y, the full and reduced regressions for the X component are represented as:

$$X_t = \sum_{k=1}^{p} A_{xx,k} \cdot X_{t-k} + \sum_{k=1}^{p} A_{xy,k} \cdot Y_{t-k} + \sum_{k=1}^{p} A_{xz,k} \cdot Z_{t-k} + \varepsilon_{x,t} \qquad (3)$$

and, with the null hypothesis in Eq. (2), we have

$$X_t = \sum_{k=1}^{p} A'_{xx,k} \cdot X_{t-k} + \sum_{k=1}^{p} A'_{xz,k} \cdot Z_{t-k} + \varepsilon'_{x,t} \,. \qquad (4)$$

According to Eqs. (3) and (4), the G-causality from Y to X, $F_{Y \to X|Z}$, is defined as

$$F_{Y \to X|Z} = \ln \frac{|\Sigma'_{xx}|}{|\Sigma_{xx}|} \,, \qquad (5)$$

where $\Sigma_{xx} = \mathrm{cov}(\varepsilon_{x,t})$, $\Sigma'_{xx} = \mathrm{cov}(\varepsilon'_{x,t})$, and $|\cdot|$ denotes the determinant of the enclosed matrix. The determinants in the numerator and the denominator in the right-hand-side of Eq. (5) are a measure of the prediction error of the model in Eq. (4) and, respectively, of the model in Eq. (3). The quantity in Eq. (5) thus measures the improvement in model fitting when the past of Y variable is included in the model for X.

As the conditioning variable Z is present in both Eqs. (3) and (4), the confounding effect of Z on the assessment of G-causality for X and Y can be eliminated. Thus, the method allows for the conditioning out of common causal influences and $F_{Y \to X|Z}$ may be read as "the degree to which the past of Y helps predict X, over and above the degree to which X is already predicted by its own past and the past of Z", see ref. (2). However, in the presence of dependencies on exogenous inputs that are not measured, as it occurs in this study because the meals directly affect glucose and NEFA concentrations, the complete elimination of the confounding effects of these inputs on the assessment of G-causality cannot be achieved. The quantities F of the type reported in Eq. (5) may

be considered as a weighted directed graph linking the vertexes X, Y and Z, and we can thus obtain a (G-)causal graph.

In summary, the type of analysis described above tries to establish whether the previous values of a time-changing variable *Y*, in our case the concentration of a metabolite or hormone, improve the prediction of another variable *X* compared to the prediction of *X* based only on its own previous values (equations (1) and (3)). This method so extends the usual notion of correlation to the stronger notion of G-causality (improved predictability of *X*, given the precedent values of *Y*). The procedure, which also holds for three or more variables, does not require assumptions about the biochemical and physiological processes involved nor to forrmulate a model that explicitly shows how the observed data are generated.

For calculating the multivariate Granger causality (MVGC) from the time series data of glucose, NEFA, insulin, C-peptide, GLP1 and GIP concentrations, we used the MVGC Matlab Toolbox implemented by Barnett and Seth (2). The experimental data were interpolated every 20 minutes using a cubic polynomial function to increase the number of time points and improve the reliability of the analysis. The order *p* of the model was assessed by the Akaike Information Criterion, which provides a balance between the goodness of fit of the model to data and the number of parameters to be estimated.

Graph indexes

The aim of the centrality measures in network analysis is that of determining the relative importance of a vertex within the graph (4). In our study, we consider two measures of centrality, degree and betweenness, and two measures typical of the network: density and efficiency.

In degree is the sum of the weights of the edges going into a node and the out degree is the sum of the weights of the edges coming out of a node. The degree of each node is the sum of its in degree and out degree. Betweenness centrality measures the extent to which a vertex lies on paths between other vertices and it is, thus, an indicator of a node's centrality in the network.

Density is the sum of the weights of the edges in the graph, divided by the number of all possible edges. Efficiency of a graph is a measure of how efficiently it exchanges information. For a weighted graph, it is defined as the sum of the minimum path lengths between variables, in proportion to the maximum efficiency of a comparable graph comprising all possible connections between variables.

The standard errors of these measures were evaluated, for each group of subjects (obese, diabetic and control) by the Bootstrap method (52).

Insulin sensitivity and secretion models

The oral glucose minimal model (9) was used to compute the insulin sensitivity (S_I) and the glucose effectiveness (S_G). We used the glucose, insulin, and C-peptide values at fasting and after the breakfast to make calculations. The indexes of β-cell sensitivity to glucose, i.e. the dynamic β-cell sensitivity, Φ_d, the static sensitivity, Φ_s, and the total sensitivity, Φ, were computed by the C-peptide minimal model as proposed by Breda et al. (5). The model parameters were estimated by minimization of a weighted least-squares index using an active-set optimization algorithm of the MATLAB library. The coefficients of variation of the estimates were found to be <20%. We validated the oral glucose minimal model in a previous study (40) by comparison with the euglycemic hyperinsulinemic clamp, which is considered the golden standard for insulin sensitivity quantification.

Robustness analysis

The robustness of the results was tested by two methods. First, we used the Bootstrap method. For each group of subjects, the resultant adjacency matrixes and the mean of the variable total degrees were computed. Second, we perturbed the time courses of the variables by an additive, zero-mean Gaussian noise. The SD of the noise was set proportional to the unperturbed value with multiplicative coefficients 0.001, 0.002, 0.005 and 0.01.The resultant adjacency matrixes and total degrees were computed.

Statistics

All of the data are expressed as mean±SEM unless otherwise specified. The Wilcoxon paired-sample test and Mann-Whitney test, followed by Bonferroni correction, were used for intragroup and intergroup comparisons, respectively. The Student's t-test was used to compare the graph indexes. Two-sided $P<0.05$ was considered significant.

RESULTS

Weight and body composition

The anthropometric data are summarized in Table 1. The patients lost a significant amount of weight after BPD. The weight loss was much more pronounced in obese subjects with normal glucose tolerance than in T2D patients. All patients lost both lean and fat mass, although the effect of bariatric surgery was stronger on fat mass reduction.

Glycated hemoglobin was significantly improved after BPD, in particular in T2D patients.

Hormonal and glucose and NEFA time courses

Figure 1 reports the time courses of plasma glucose, NEFA, C-peptide, insulin, GLP1 and GIP concentrations in obese normoglycemic patients before and after BPD (A), in obese T2D patients before and after BPD (B), and in both controls and patients after gastro-intestinal surgery (C).

Granger causality

Before the graph analysis, we have implemented the Granger causality model to find the time-lagged causal connectivity among the time-series available. The model order was 10 for obese and diabetic subjects and 8 for controls. In this way, we have obtained the weighted adjacency matrix that gives the most probable, non-trivial, weights of the edges joining pairs of vertices in the graph (Figure 2, left column). Adjacencies are all nonzero only in controls.

Graph analysis

In the networks reported in Figure 2 (right column), the time-series variables represent the nodes and the significant connections obtained using the Granger correlations are the weighted edges. The value of the betweenness of a node is indicated by a color. The dominant variable/s have

a red color. As soon as the dominance of betweenness becomes less strong, the color is lighter, from orange to yellow. Some of the hedges are unidirectional, as also shown by the adjacency matrixes.

In the obese subjects before bariatric surgery NEFA have the strongest influence on the other variables while, after surgery, GLP1 and C-peptide, i.e., the insulin secretion, play a central role. Also in the obese diabetic subjects, NEFA dominates over the other variables, but after bariatric surgery, GLP1 controls the system. In the healthy controls, finally, NEFA, GLP1 and C-peptide have a comparable relevance in the network.

Table 2 reports the numerical values of the betweenness (also shown by the color code in Figure 2, right column), of the in degrees, out degrees, as well as the total degrees of the network for plasma glucose, NEFA, insulin, C-peptide, GLP1 and GIP in obese and T2D subjects before and after surgery, and in control subjects. The values of the in degrees in Table 2 equal the sum (divided by 5, i.e. the maximal number of edges reaching a node) of the elements in the corresponding rows of the weighted adjacency matrix of Figure 2. Glucose in degree, for instance, is the sum (divided by 5) of entries of the first row of adjacency matrix, as seen from the numerical values shown in Figure 1 of the Appendix. Similarly, the values of out degrees equal the sum of elements in the corresponding columns of the weighted adjacency matrix. After surgery, the betweenness of all variables changes significantly, or tends to change, in the same direction in both obese and diabetic subjects (for instance, downwards in NEFA and upwards in GLP1). The betweenness of all variables does not differ significantly between controls and obese subjects post BPD, while, in diabetic subjects, the betweenness of GLP1 remains significantly lower than that of controls.

In obese subjects, the in degrees increase significantly for C-peptide, GLP1 and GIP while decrease for glucose and insulin; the out degrees diminish only for NEFA and insulin, and raise only for GIP. No significant differences occur between obese post BPD and controls. Total degrees significantly increase post BPD for C-peptide, GLP1 and GIP. On the contrary, they decrease for

glucose, NEFA and insulin. However, the total degrees of insulin and GLP1 remain lower compared with those of controls.

In diabetic subjects, the in degrees decrease for insulin and C-peptide and increase for GLP1, the out degrees lower for glucose, insulin and C-peptide and heighten for NEFA and GLP1; the out degrees of NEFA are still significantly different from those of controls. Total degrees of NEFA and GLP1 increase post BPD. Conversely, total degrees of glucose and insulin decrease after surgery. Only the insulin and GIP degrees remain significantly lower compared with controls.

Although the changes of degrees after surgery do not present a clear-cut pattern, in both obese and diabetic subjects the total degrees decrease in glucose and insulin, and increase in GLP1.

The graph density significantly increases after surgery in the obese subjects (Student's t-test=8.32, $P<0.001$) and the graph efficiency increases (t=5.64, $P<0.001$). In T2D subjects, graph efficiency significantly increases (t=7.62, $P<0.001$) post BPD, while the graph density remains unchanged. The graph efficiency in obese and diabetic subjects post BPD is similar to the efficiency in controls (P=NS). Conversely, the graph density in controls remains higher than the density in obese and diabetic subjects after surgery (t=4.05 $P<0.005$ and t=4.06 $P<0.005$, respectively).

Insulin sensitivity and secretion

Table 1 reports S_I, S_G and cumulative insulin secretion (AUC_{ISR}).

Insulin sensitivity increases more than 5 times in obese and 4 times in T2D subjects after BPD, matching the values observed in healthy controls. The cumulative insulin secretion decreases significantly in T2D subjects after BPD and even halves in obese subjects.

Robustness analysis

The adjacency matrixes computed by the Bootstrap method were marginally changed with respect to those shown in Fig. 2. The degrees computed by this method were not significantly different from those reported in Table 2. When the Granger analysis was applied to the time-course

294 of the variables perturbed by noise the total degrees tended to decrease, but the difference of total
295 degrees from before to after BPD remained rather stable as shown in the Figure 2 of the Appendix,
296 so the changes from before to after BPD reflect substantially those in Table 2.

297

DISCUSSION

In his study, we set up a graphical approach that models, identifies and visualizes the causal relationships between the components of data recorded during a 24-hour multi-meal test. Glucose, insulin, C-peptide, NEFA, GLP-1 and GIP concentrations were measured in T2D and in obese normoglycemic subjects, before and after malabsorptive metabolic surgery, and in healthy controls.

Data were analyzed by the Granger causality method and graph analysis, which are widely used for instance in exploring multivariate time series of economic data (8) and brain networks (11). Our analysis permitted to establish the degree of association among the metabolic and hormonal time-series in a manner that allows identification of the network of strongest associations. The magnitude of the combined associations is measured by two indexes that are related to certain concepts of graph theory, i.e. the density of nodes and the efficiency of the network. These indexes are used to identify the degree of interaction among the variables and they provide a quantitative basis for grouping energy substrates and hormones.

The Granger and graph methods do not require a model that describes the underlying physiology of the glucose-insulin system, and use all the recorded data simultaneously to reveal the mutual influences among the variables recorded. Therefore, it may capture features in response to the meals that are hardly detectable by a particular mathematical model.

Limitations of our study are that Granger causality is a statistical inference on the relationships among variables but do not necessarily imply physical causality which needs to be determined by an interventional experiment. However, the introduction of causality rules, as in the Granger causality, may provide a means to distinguish whether any of our variables interact directly or whether the appearance of a correlation is a result of chance or the variables are forced by a common third variable. Another limitation is the lack of data on glucagon concentrations, which is a major player in type 2 diabetes with GIP increasing glucagon circulating levels in type 2 diabetes (43). Finally, we stress that the use of splines to interpolate our hourly data might bias the analysis. Rapidly occurring phenomena, such as the early phase of insulin response after initiating a meal,

may indeed be missed because of the spline approximation that produces a smoothing in the time-course of the variables

To investigate a complex system such as that of the *in vivo* glucose metabolic control as a whole, it is important to study how hormones and energy substrates are connected. The components of the glucose system and their interactions are best characterized as a network, and they are conveniently represented as a graph where nodes are connected with edges.

Our analysis shows that NEFA is the most strongly connected variable in the network system of both obese and diabetic subjects at the baseline. Plasma NEFA are produced by the hydrolysis of triglycerides (TG) stored in the adipose tissue, however after a meal dietary TG are hydrolyzed in the circulatory stream by lipoprotein lipase (LPL) and the proportion escaping in the so-called spillover process joins the plasma NEFA pool (14). In insulin resistant individuals, fat mobilization is not efficiently suppressed by insulin. NEFA concentrations are associated acutely with insulin resistance reducing insulin-mediated glucose uptake (3, 44), increasing hepatic gluconeogenesis (38, 45) and reducing hepatic insulin clearance (51).

BPD is a mainly malabsorptive metabolic operation that greatly reduces lipid absorption and, thus, its action in improving insulin sensitivity might depend on the reduction of circulating levels of NEFA. However, here we show that it is the increase in GLP1 plasma levels, rather than the reduction of NEFA circulating levels, which drives the reduction of plasma glucose and insulin over 24 hours. Rather than finding a reduction of plasma NEFA we found unchanged or sometime slightly increased levels. Fasting and low energy intake are associated with increased circulating levels of NEFA. In fact, the highest plasma NEFA concentrations are observed after an overnight fast, with suppression after each meal (37, 27, 39). During energy deprivation, adipose tissue lipolysis is increased with generation of fatty acids and glycerol, which are released into the circulatory stream for use by other organs as energy substrates. Food deprivation in rats is associated with doubled hormone sensitive lipase protein expression and activity in the adipose

tissue (46). After bariatric surgery it was reported that all lipids in tissues and plasma diminished except plasma NEFA, which maintained higher levels than controls (35). Therefore, NEFA plasma levels remained elevated after bariatric surgery due to energy intake restriction and weight loss.

In addition, the high plasma levels of GIP observed in T2D subjects at baseline were detrimental for their glucose metabolism. GIP signaling, in fact, promotes fat accumulation in experimental animals (19, 22, 23, 24, 26, 33). Obese humans also hyper-secrete GIP (10, 13) suggesting that GIP may promote obesity in humans. GIP receptor knockout rodents are protected from obesity-related diabetes (32), as well animals genetically engineered to lack K cells also resist development of high fat diet-induced obesity and insulin resistance without any collateral serious adverse effect (1). Furthermore, chronic administration of (Pro^3GIP), a specific and stable GIP receptor antagonist, can prevent or reverse many of the established metabolic alterations, including insulin resistance, observed in type 2 diabetes (15).

In the present study, both T2D and normoglycemic obese patients had the normalization of insulin resistance just 1 month after BPD. In addition, glycated hemoglobin was drastically reduced after BPD in T2D patients (Table 1). Likewise, a very low calorie diet administered to T2D patients for 1 month was effective in improving glycated hemoglobin (20).

In conclusion, increased GLP1 circulating levels over 24 hours positively impact on glucose homeostasis in both obese and obese diabetic individuals who underwent a malabsorptive operation. The reduction of plasma GIP also contributed to the improvement of glucose metabolism. It is possible that the combination of a pharmaceutical treatment reducing GIP and increasing GLP1 plasma levels will contribute to a better glycemic control in type 2 diabetes. Indeed, recent findings (48) show that an approach based on triple hormone therapy (GLP1, peptide YY and oxyntomodulin) is likely to be a useful tool against obesity.

373 The application of Granger causality and graph analyses shed new light on the patho-
374 physiology of gastro-intestinal surgery and on glycemic control, and it opens a new avenue to the
375 use of these computational techniques in metabolic studies.

376

ACKNOWLEDGMENTS

Author contributions

E.P., S.S., A.B. wrote the manuscript. S.S and E.P. analyzed the data. E.C. searched data and made the study. S.B. reviewed/edited the manuscript. G.M. designed the study and contributed to writing the manuscript. Guarantors are S.S., A.B. and G.M.

All the authors declare no conflict of interest.

The study was supported by internal funds of the Catholic University.

401 **REFERENCES**

402 1. Althage MC, Ford EL, Wang S, Tso P, Polonsky KS, Wice BM. Targeted ablation of
403 glucose-dependent insulinotropic polypeptide-producing cells in transgenic mice reduces
404 obesity and insulin resistance induced by a high fat diet. J Biol Chem 283: 18365–18376,
405 2008.
406 2. Barnett L, Seth AK. The MVGC multivariate Granger causality toolbox: a new approach to
407 Granger-causal inference. J Neurosci Methods 223: 50–68, 2014.
408 3. Boden G, Chen X, Ruiz J, White JV, Rossetti L. Mechanisms of fatty acid-induced
409 inhibition of glucose uptake. J Clin Invest 93: 2438–2446, 1994.
410 4. Bollobas B. *Modern Graph Theory*. New York: Springer, 1998.
411 5. Breda E, Cavaghan MK, Toffolo G, Polonsky KS, Cobelli C. Oral glucose tolerance test
412 minimal model indexes of beta-cell function and insulin sensitivity. Diabetes 50: 150–158,
413 2001.
414 6. Carpentier A, Mittelman SD, Bergman RN, Giacca A, Lewis GF. Prolonged elevation of
415 plasma free fatty acids impairs pancreatic beta-cell function in obese nondiabetic humans
416 but not in individuals with type 2 diabetes. Diabetes 49: 399–408, 2000.
417 7. Carpentier A, Mittelman SD, Lamarche B, Bergman RN, Giacca A, Lewis GF. Acute
418 enhancement of insulin secretion by FFA in humans is lost with prolonged FFA elevation.
419 Am J Physiol 276: E1055–E1066, 1999.
420 8. Castagneto-Gissey G, Chavez M, De Vico Fallani F. Dynamic Granger-causal networks of
421 electricity spot prices: A novel approach to market integration. Energy Econ 44: 422–432,
422 2014.
423 9. Caumo A, Bergman RN, Cobelli C. Insulin sensitivity from meal tolerance tests in normal
424 subjects: a minimal model index. J Clin Endocrinol Metab 85: 4396–4402, 2000.
425 10. Creutzfeldt W, Ebert R, Willms B, Frerichs H, Brown JC. Gastric inhibitory polypeptide
426 (GIP) and insulin in obesity: increased response to stimulation and defective feedback
427 control of serum levels. Diabetologia 14: 15–24, 1978.

11. De Vico Fallani F, Astolfi L, Cincotti F, Mattia D, Tocci A, Salinari S, Marciani MG, Witte H, Colosimo A, Babiloni F. Brain network analysis from high-resolution EEG recordings by the application of theoretical graph indexes. IEEE Trans Neural Syst Rehabil Eng 16: 442–452, 2008.
12. Dixon JB, O'Brien PE, Playfair J, Chapman L, Schachter LM, Skinner S, Proietto J, Bailey M, Anderson M. Adjustable gastric banding and conventional therapy for type 2 diabetes: a randomized controlled trial. JAMA 299: 316–323, 2008.
13. Ebert R, Frerichs H, Creutzfeldt W. Impaired feedback control of fat induced gastric inhibitory polypeptide (GIP) secretion by insulin in obesity and glucose intolerance. Eur J Clin Invest 9: 129–135, 1979.
14. Evans K, Burdge GC, Wootton SA, Clark ML, Frayn KN. Regulation of dietary fatty acid entrapment in subcutaneous adipose tissue and skeletal muscle. Diabetes 51: 2684–2690, 2002.
15. Gault VA, O'Harte FP, Harriott P, Flatt PR. Characterization of the cellular and metabolic effects of a novel enzyme-resistant antagonist of glucose-dependent insulinotropic polypeptide. Biochem Biophys Res Commun 290: 1420–1426, 2002.
16. Granger CWJ. Investigating causal relations by econometric models and cross-spectral methods. Econometrica 37: 424–438, 1969.
17. Guidone C, Manco M, Valera-Mora E, Iaconelli A, Gniuli D, Mari A, Nanni G, Castagneto M, Calvani M, Mingrone G. Mechanisms of recovery from type 2 diabetes after malabsorptive bariatric surgery. Diabetes 55: 2025–2031, 2006.
18. Hainer V, Toplak H, Mitrakou A. Treatment modalities of obesity: what fits whom? Diabetes Care 31: S269–S277, 2008.
19. Hansotia T, Maida A, Flock G, Yamada Y, Tsukiyama K, Seino Y, Drucker DJ. Extrapancreatic incretin receptors modulate glucose homeostasis, body weight, and energy expenditure. J Clin Invest 117: 143–152, 2007.

20. Henry RR, Wiest-Kent TA, Scheaffer L, Kolterman OG, Olefsky JM. Metabolic consequences of very-low-calorie diet therapy in obese non-insulin-dependent diabetic and nondiabetic subjects. Diabetes 35: 155-164, 1986.
21. International Diabetes Federation. IDF Diabetes Atlas. Epidemiology and Morbidity. In: International Diabetes Federation. Available from http://www.idf.org/
22. Irwin N, Flatt PR. Evidence for beneficial effects of compromised gastric inhibitory polypeptide action in obesity-related diabetes and possible therapeutic implications. Diabetologia 52: 1724–1731, 2009.
23. Isken F, Pfeiffer AF, Nogueiras R, Osterhoff MA, Ristow M, Thorens B, Tschöp MH, Weickert MO. Deficiency of glucose-dependent insulinotropic polypeptide receptor prevents ovariectomy-induced obesity in mice. Am J Physiol Endocrinol Metab 295: E350–E355, 2008.
24. Joo E, Harada N, Yamane S, Fukushima T, Taura D, Iwasaki K, Sankoda A, Shibue K, Harada T, Suzuki K, Hamasaki A, Inagaki N. Inhibition of gastric inhibitory polypeptide receptor signaling in adipose tissue reduces insulin resistance and hepatic steatosis in high fat diet-fed mice. Diabetes pii: db160758, 2017.
25. Knowler WC, Barrett-Connor E, Fowler SE, Hamman RF, Lachin JM, Walker EA, Nathan DM; Diabetes Prevention Program Research Group. Reduction in the incidence of type 2 diabetes with lifestyle intervention or metformin. N Engl J Med 346: 393–403, 2002.
26. Kruse M, Keyhani-Nejad F, Isken F, Nitz B, Kretschmer A, Reischl E, de las Heras Gala T, Osterhoff MA, Grallert H, Pfeiffer AF. High-fat diet during mouse pregnancy and lactation targets GIP-regulated metabolic pathways in adult male offspring. Diabetes 65: 574–584, 2016.
27. Kruszynska YT, Munro J, Home PD, McIntyre N. Twenty-four hour C-peptide and insulin secretion rates and diurnal profiles of glucose, lipids and intermediary metabolites in cirrhosis. Clin Sci (Lond) 83: 597–605, 1992.

480 28. Lewis GF, Carpentier A, Adeli K, Giacca A. Disordered fat storage and mobilization in the
481 pathogenesis of insulin resistance and type 2 diabetes. Endocr Rev 23: 201–229, 2002.
482 29. Marceau P, Hould FS, Potvin M, Lebel S, Biron S. Biliopancreatic diversion (duodenal
483 switch procedure). Eur J Gastroenterol Hepatol 11: 99–103, 1999.
484 30. Mingrone G, Manco M, Granato L, Calvani M, Scarfone A, Mora EV, Greco AV, Vidal H,
485 Castagneto M, Ferrannini E. Leptin pulsatility in formerly obese women. FASEB J 19:
486 1380–1382, 2005.
487 31. Mingrone G, Panunzi S, De Gaetano A, Guidone C, Iaconelli A, Leccesi L, Nanni G, Pomp
488 A, Castagneto M, Ghirlanda G, Rubino F. Bariatric surgery versus conventional medical
489 therapy for type 2 diabetes. N Engl J Med 366: 1577–1585, 2012.
490 32. Miyawaki K, Yamada Y, Ban N, Ihara Y, Tsukiyama K, Zhou H, Fujimoto S, Oku A, Tsuda
491 K, Toyokuni S, Hiai H, Mizunoya W, Fushiki T, Holst JJ, Makino M, Tashita A, Kobara Y,
492 Tsubamoto Y, Jinnouchi T, Jomori T, Seino Y. Inhibition of gastric inhibitory polypeptide
493 signaling prevents obesity. Nat Med 8: 738–742, 2002.
494 33. Nie Y, Ma RC, Chan JC, Xu H, Xu G. Glucose-dependent insulinotropic peptide impairs
495 insulin signaling via inducing adipocyte inflammation in glucose-dependent insulinotropic
496 peptide receptor-overexpressing adipocytes. FASEB J 26: 2383–2393, 2012.
497 34. Overweight and obesity statistics. U.S. Department of Health and Human Services NIDDK.
498 http://www.niddk.nih.gov/health-information/health-statistics/Documents/stat904z.pdf
499 35. Pardina E, Lecube A, Llamas R, Catalán R, Galard R, Fort JM, Allende H, Vargas V,
500 Baena-Fustegueras JA, Peinado-Onsurbe J. Lipoprotein lipase but not hormone-sensitive
501 lipase activities achieve normality after surgically induced weight loss in morbidly obese
502 patients. Obes Surg 19: 1150–1158, 2009.
503 36. Pories WJ, MacDonald KG. The surgical treatment of morbid obesity. Curr Opin Gen Surg
504 195–205, 1993.

505 37. Reaven GM, Hollenbeck C, Jeng C-Y, Wu MS, Chen Y-DI. Measurement of plasma
506 glucose, free fatty acid, lactate, and insulin for 24 h in patients with NIDDM. Diabetes 37:
507 1020–1024, 1988.
508 38. Roden M, Stingl H, Chandramouli V, Schumann WC, Hofer A, Landau BR, Nowotny P,
509 Waldhäusl W, Shulman GI. Effects of free fatty acid elevation on postabsorptive
510 endogenous glucose production and gluconeogenesis in humans. Diabetes 49:701–707,
511 2000.
512 39. Ruge T, Hodson L, Cheeseman J, Dennis AL, Fielding BA, Humphreys SM, Frayn KN,
513 Karpe F. Fasted to fed trafficking of Fatty acids in human adipose tissue reveals a novel
514 regulatory step for enhanced fat storage. J Clin Endocrinol Metab 94: 1781–1788, 2009.
515 40. Salinari S, Bertuzzi A, Asnaghi S, Guidone C, Manco M, Mingrone G. First-phase insulin
516 secretion restoration and differential response to glucose load depending on the route of
517 administration in type 2 diabetic subjects after bariatric surgery. Diabetes Care 32: 375–380,
518 2009.
519 41. Schauer PR, Bhatt DL, Kirwan JP, Wolski K, Brethauer SA, Navaneethan SD, Aminian A,
520 Pothier CE, Kim ES, Nissen SE, Kashyap SR; STAMPEDE Investigators. Bariatric surgery
521 versus intensive medical therapy for diabetes--3-year outcomes. N Engl J Med 370: 2002–
522 2013, 2014.
523 42. Scopinaro N, Gianetta E, Civalleri D, Bonalumi U, Bachi V. Bilio-pancreatic bypass for
524 obesity. II. Initial experience in man. Br J Surg 66: 618–620, 1979.
525 43. Shah P, Vella A, Basu A, Basu R, Schwenk WF, Rizza RA. Lack of suppression of
526 glucagon contributes to postprandial hyperglycemia in subjects with type 2 diabetes
527 mellitus. J Clin Endocrinol Metab 85: 4053–4059, 2000.
528 44. Shah P, Vella A, Basu A, Basu R, Adkins A, Schwenk WF, Johnson CM, Nair KS, Jensen
529 MD, Rizza RA. Effects of free fatty acids and glycerol on splanchnic glucose metabolism
530 and insulin extraction in nondiabetic humans. Diabetes 51: 301–310, 2002.

45. Staehr P, Hother-Nielsen O, Landau BR, Chandramouli V, Holst JJ, Beck-Nielsen H. Effects of free fatty acids per se on glucose production, gluconeogenesis, and glycogenolysis. Diabetes 52: 260–267, 2003.
46. Sztalryd C, Kraemer FB. Regulation of hormone sensitive lipase during fasting. Am J Physiol 266**:** E179–E185, 1994.
47. Tam CS, Berthoud HR, Bueter M, Chakravarthy MV, Geliebter A, Hajnal A, Holst J, Kaplan L, Pories W, Raybould H, Seeley R, Strader A, Ravussin E. Could the mechanisms of bariatric surgery hold the key for novel therapies? report from a Pennington Scientific Symposium. Obes Rev 12: 984–994, 2011.
48. Tan T, Behary P, Tharakan G, Minnion J, Al-Najim W, Wewer Albrechtsen NJ, Holst JJ, Bloom SR. The effect of a subcutaneous infusion of GLP-1, OXM and PYY on Energy intake and Expenditure in Obese volunteers. J Clin Endocrinol Metab 2017, to appear. doi: 10.1210/jc.2017-00469.
49. Tuomilehto J, Lindström J, Eriksson JG, Valle TT, Hämäläinen H, Ilanne-Parikka P, Keinänen-Kiukaanniemi S, Laakso M, Louheranta A, Rastas M, Salminen V, Uusitupa M; Finnish Diabetes Prevention Study Group. Prevention of type 2 diabetes mellitus by changes in lifestyle among subjects with impaired glucose tolerance. N Engl J Med 344: 1343–1350, 2001.
50. van Dam RM, Willett WC, Rimm EB, Stampfer MJ, Hu FB. Dietary fat and meat intake in relation to risk of type 2 diabetes in men. Diabetes Care 25: 417–424, 2002.
51. Wiesenthal SR, Sandhu H, McCall RH, Tchipashvili V, Yoshii H, Polonsky K, Shi ZQ, Lewis GF, Mari A, Giacca A. Free fatty acids impair hepatic insulin extraction in vivo. Diabetes 48: 766–774, 1999.
52. Wu C.F.J. Jackknife, bootstrap and other resampling methods in regression analysis (with discussions). Ann Statist 14: 1261–1350, 1986.

Figure legends

Figure 1

Time course of plasma glucose, insulin, C-peptide, GLP1, NEFA and GIP concentrations in obese patients at baseline (black lines) and at 1 month after BPD (red lines) (panel A), in diabetic patients at baseline (black) and at 1 month after BPD (red) (panel B), and in both controls (black bold lines) and surgical patients (blue for obese and green for diabetic subjects) at 1 month after BPD (panel C). The vertical lines indicate the meal times. Concentration values are mean ± SE.

Figure 2

Adjacency matrixes (left column) and betweenness centrality indexes (right column) of the graphs in obese and diabetic patients pre and post BPD and in control subjects. The numbers from 1 to 6 indicate plasma glucose, NEFA, insulin, C-peptide, GLP1 and GIP, respectively. The colors, from yellow for lowest value to red for highest value, represent the values of the variables (weighted adjacency in the matrixes and betweenness in the nodes of the graph). Note that the color scale is different in the various panels.

575 **Table 1**. Anthropometric and metabolic parameters of controls and of the obese and diabetic
576 patients at baseline and at 1 month after BPD.

577 Significances: * indicates a significant difference (P<0.05) between variables in controls vs. patients
578 post BPD, and # indicates a significant difference (P<0.05) between variables in patients before and
579 after BPD.

580

581

Parameters	*Obese subjects pre BPD*	*Obese subjects post BPD*	*Diabetic subjects pre BPD*	*Diabetic subjects post BPD*	*Controls*
Weight kg	131.10 ± 7.79	118.05 ± 7.91$^{\#,*}$	134.60 ± 8.15	124.42 ± 9.14$^{\#*}$	72.10 ± 2.66
BMI kg m^{-2}	46.77 ± 2.29	42.15 ± 2.47$^{\#,*}$	45.29 ± 2.23	41.56 ± 2.59$^{\#*}$	26.46 ± 0.49
FFM kg	70.89 ± 4.71	67.31 ± 5.66*	76.60 ± 6.97	74.12 ± 6.87$^{\#*}$	50.68 ± 4.25
FM kg	60.19 ± 4.29	50.73 ± 3.91$^{\#,*}$	59.20 ± 5.27	53.64 ± 0.56$^{\#*}$	21.42 ± 2.18
HbA1c %	5.98 ± 0.31	5.00 ± 0.45$^{\#}$	11.88 ± 1.53*	7.71 ± 0.74$^{\#*}$	5.04 ± 0.36
$S_G \times 10^2$ min^{-1}	4.20 ± 0.26	3.81 ± 0.16	2.96 ± 0.49	3.84 ± 0.44	3.74±0.21
$S_I \times 10^4$ min^{-1}pM^{-1}	0.317 ± 0.06	1.70 ± 0.27$^{\#}$	0.322 ± 0.09	1.28 ± 0.18$^{\#}$	1.44±0.23
AUC_{ISR} nmol	42.83±8.30	21.05±5.21$^{\#}$	29.67±6.3$^{\#}$	23.59±7.9	20.45±2.76
$\Phi_s \times 10^9$ min^{-1}	25.3±6.59	43.35±6.21$^{\#}$	12.81±3.16	40.9±6.35$^{\#}$	35.7±5.9
$\Phi_d \times 10^9$	739.96±202.71	383.81±106.25$^{\#}$	684.45±216.93	525.46±155.46	401.6±108.7
$\Phi \times 10^9$ min^{-1}	33.91±6.1	47.7±10.1$^{\#}$	20.9±3.43	46.6±6.51$^{\#}$	40.7±5.8

582

583

584 **Table 2.** Graph theory and network analysis of the interactions among glucose, NEFA, insulin, C-
585 peptide, GIP and GLP1 (mean ± SD).

586 Significances: * post BPD vs pre BPD $P<0.05$, ° post BPD vs controls $P<0.05$.

Obese subjects	***Glucose***	***NEFA***	***Insulin***	***C-peptide***	***GLP1***	***GIP***
Betweenness pre	0.21±0.14	0.78±0.14	0.35±0.14	0.06±0.07	0.24±0.14	0.80±0.21
Betweenness post	0.32±0.14	0.03±0.07*	0.50±0.21	0.19±0.07*	0.39±0.14*	0.24±0.07*
In degree pre	0.095±0.009	0.069±0.010	0.062±0.010	0.043±0.012	0.079±0.010	0.062±0.013
In degree post	0.052±0.008*	0.065±0.009	0.033±0.008*	0.081±0.022*	0.145±0.015*	0.110±0.018*
Out degree pre	0.051±0.009	0.097±0.008	0.071±0.013	0.060±0.008	0.069±0.011	0.063±0.007
Out degree post	0.058±0.013	0.064±0.008*	0.057±0.010*	0.055±0.016	0.076±0.011	0.178±0.011*
Degree pre	0.146±0.015	0.167±0.012	0.133±0.018	0.103±0.018	0.148±0.016	0.125±0.015
Degree post	0.110±0.017*°	0.130±0.014*	0.089±0.016*°	0.136±0.035*	0.221±0.021*°	0.288±0.025*
Diabetic subjects	***Glucose***	***NEFA***	***Insulin***	***C-peptide***	***GLP1***	***GIP***
Betweenness pre	0.12±0.28	0.73±0.21	0.03±0.07	0.12±0.14	0.06±0.07	0.18±0.14
Betweenness post	0.24±0.21	0.01±0.07*	0.13±0.14*	0.21±0.21	0.14±0.14*°	0.13±0.14
In degree pre	0.066±0.017	0.151±0.023	0.115±0.017	0.109±0.009	0.085±0.009	0.088±0.017
In degree post	0.079±0.010*	0.149±0.028	0.077±0.013*	0.070±0.015*	0.136±0.019*	0.083±0.018
Out degree pre	0.108±0.014	0.075±0.014	0.113±0.008	0.114±0.016	0.112±0.016	0.091±0.012
Out degree post	0.058±0.015*	0.172±0.014*°	0.063±0.017*	0.079±0.020*	0.138±0.016*	0.084±0.020
Degree pre	0.175±0.028	0.226±0.034	0.228±0.018	0.223±0.015	0.197±0.019	0.179±0.023
Degree post	0.137±0.017*	0.321±0.034*	0.140±0.023*°	0.150±0.032*	0.274±0.029*	0.166±0.032°
Controls	***Glucose***	***NEFA***	***Insulin***	***C-peptide***	***GLP1***	***GIP***
Betweenness	0.45±0.14	0.07±0.14	0.15±0.14	0.13±0.14	0.59±0.14	0.06±0.07
In degree	0.095±0.031	0.110±0.038	0.112±0.037	0.071±0.026	0.169±0.015	0.111±0.020
Out degree	0.115±0.026	0.077±0.034	0.107±0.027	0.104±0.018	0.144±0.025	0.120±0.023
Degree	0.210±0.043	0.187±0.048	0.219±0.037	0.175± 0.038	0.313±0.023	0.231±0.027

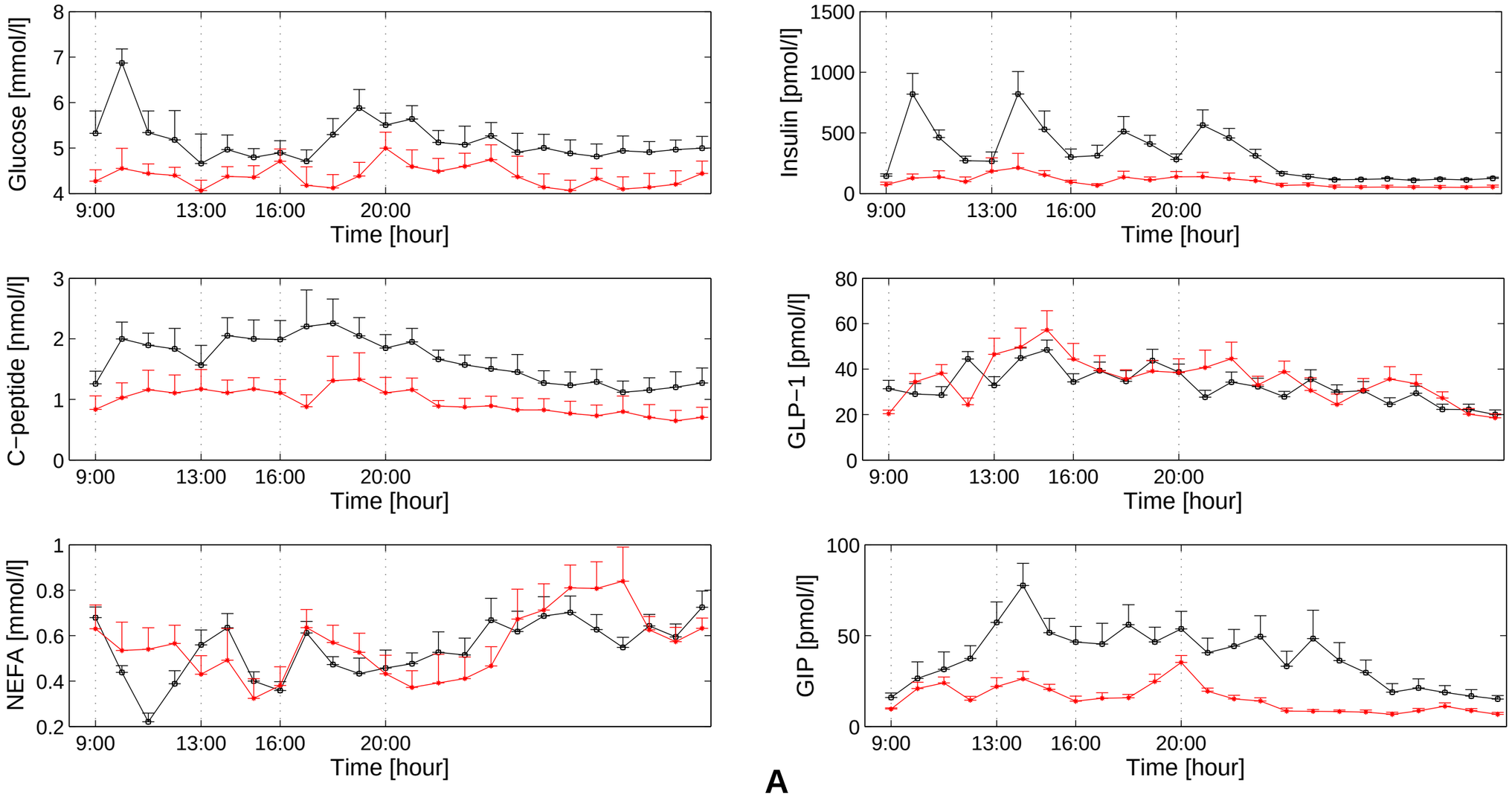
Glucose [mmol/l]
8
7
6
5
4
9:00
13:00
16:00
20:00
Time [hour]
Insulin [pmol/l]
1500
1000
500
0
9:00
13:00
16:00
20:00
Time [hour]
C−peptide [nmol/l]
3
2
1
0
9:00
13:00
16:00
20:00
Time [hour]
GLP−1 [pmol/l]
80
60
40
20
0
9:00
13:00
16:00
20:00
Time [hour]
NEFA [mmol/l]
1
0.8
0.6
0.4
0.2
9:00
13:00
16:00
20:00
Time [hour]
GIP [pmol/l]
100
50
0
9:00
13:00
16:00
20:00
Time [hour]

A

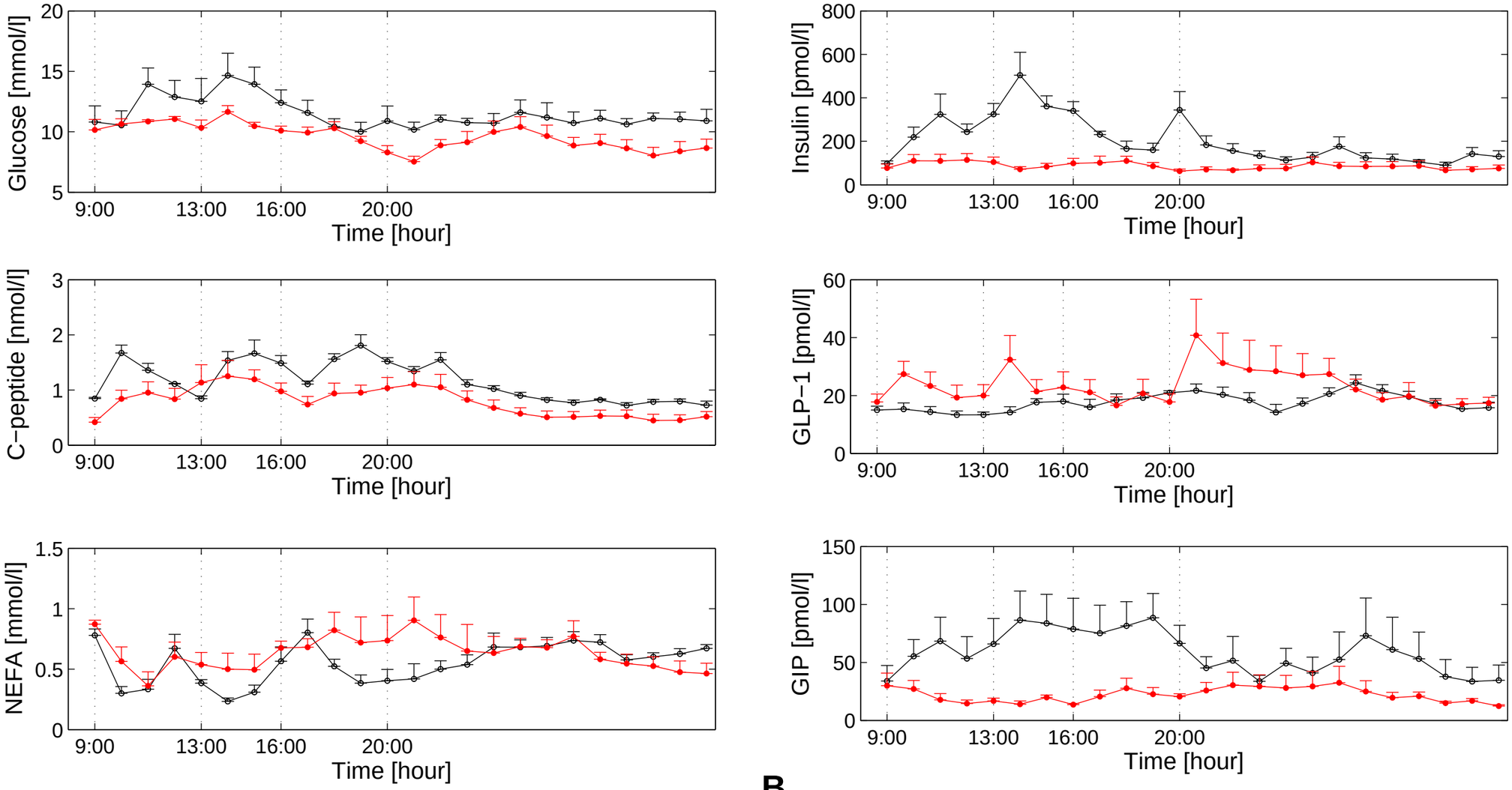
Glucose [mmol/l]
20
15
10
5
9:00
13:00
16:00
20:00
Time [hour]
Insulin [pmol/l]
800
600
400
200
0
9:00
13:00
16:00
20:00
Time [hour]
C−peptide [nmol/l]
3
2
1
0
9:00
13:00
16:00
20:00
Time [hour]
GLP−1 [pmol/l]
60
40
20
0
9:00
13:00
16:00
20:00
Time [hour]
NEFA [mmol/l]
1.5
1
0.5
0
9:00
13:00
16:00
20:00
Time [hour]
GIP [pmol/l]
150
100
50
0
9:00
13:00
16:00
20:00
Time [hour]

B

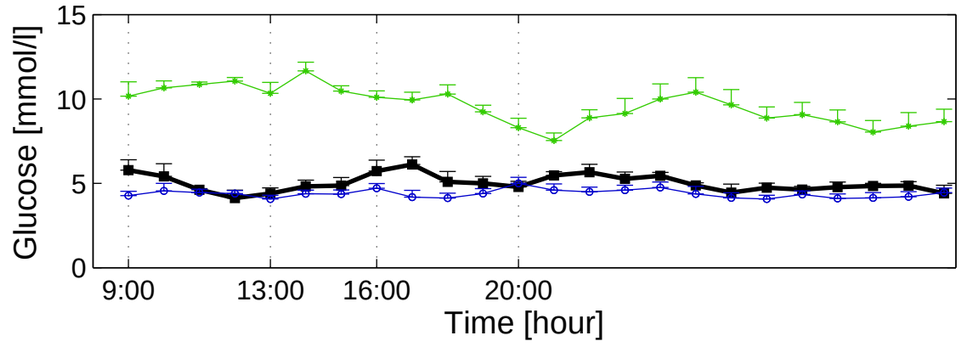
Glucose [mmol/l]
15
10
5
0
9:00
13:00
16:00
20:00
Time [hour]

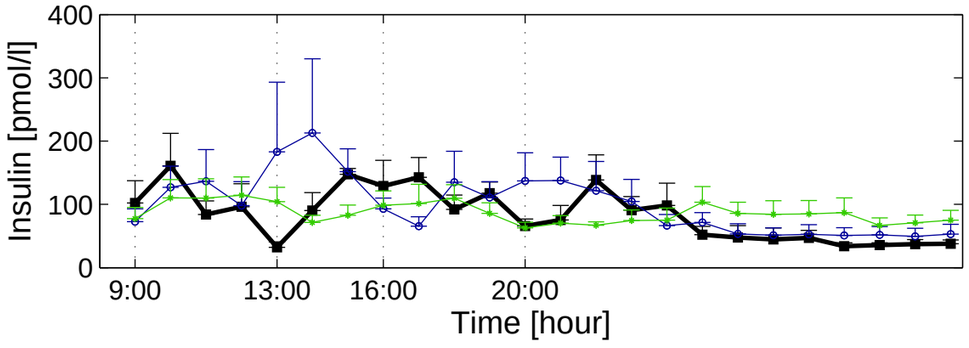
Insulin [pmol/l]
400
300
200
100
0
9:00
13:00
16:00
20:00
Time [hour]

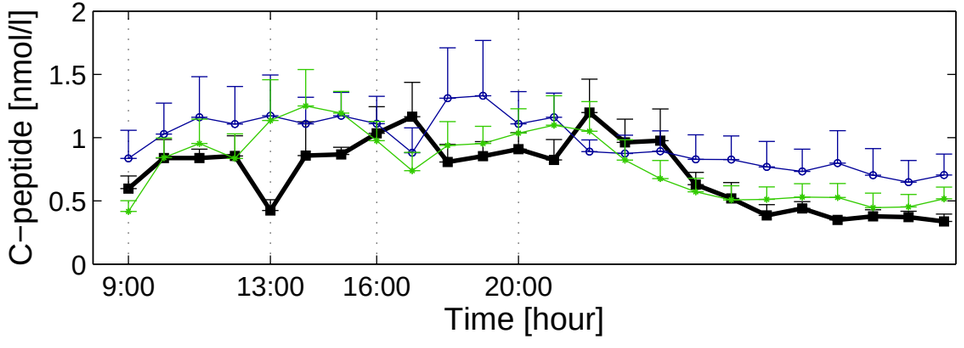
C−peptide [nmol/l]
2
1.5
1
0.5
0
9:00
13:00
16:00
20:00
Time [hour]

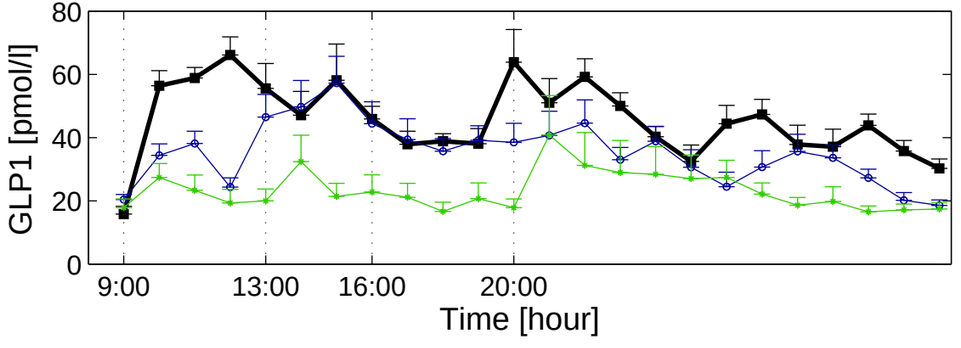
GLP1 [pmol/l]
80
60
40
20
0
9:00
13:00
16:00
20:00
Time [hour]

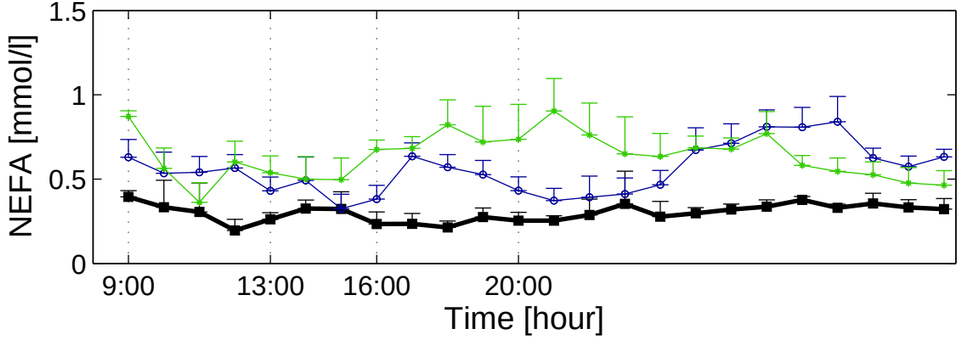
NEFA [mmol/l]
1.5
1
0.5
0
9:00
13:00
16:00
20:00
Time [hour]

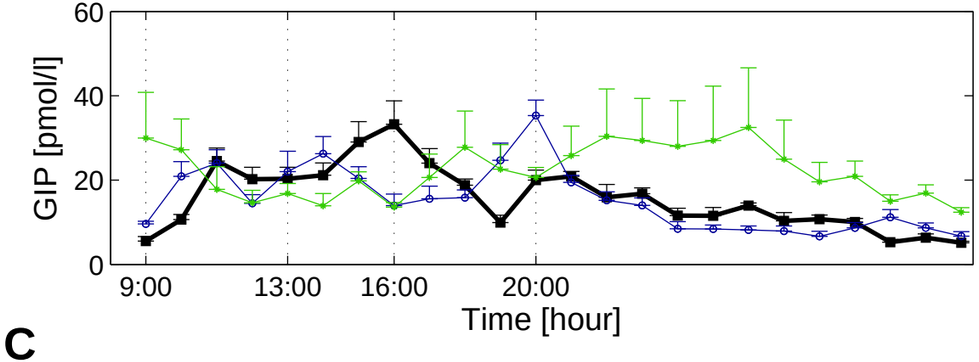
GIP [pmol/l]
60
40
20
0
9:00
13:00
16:00
20:00
Time [hour]

C

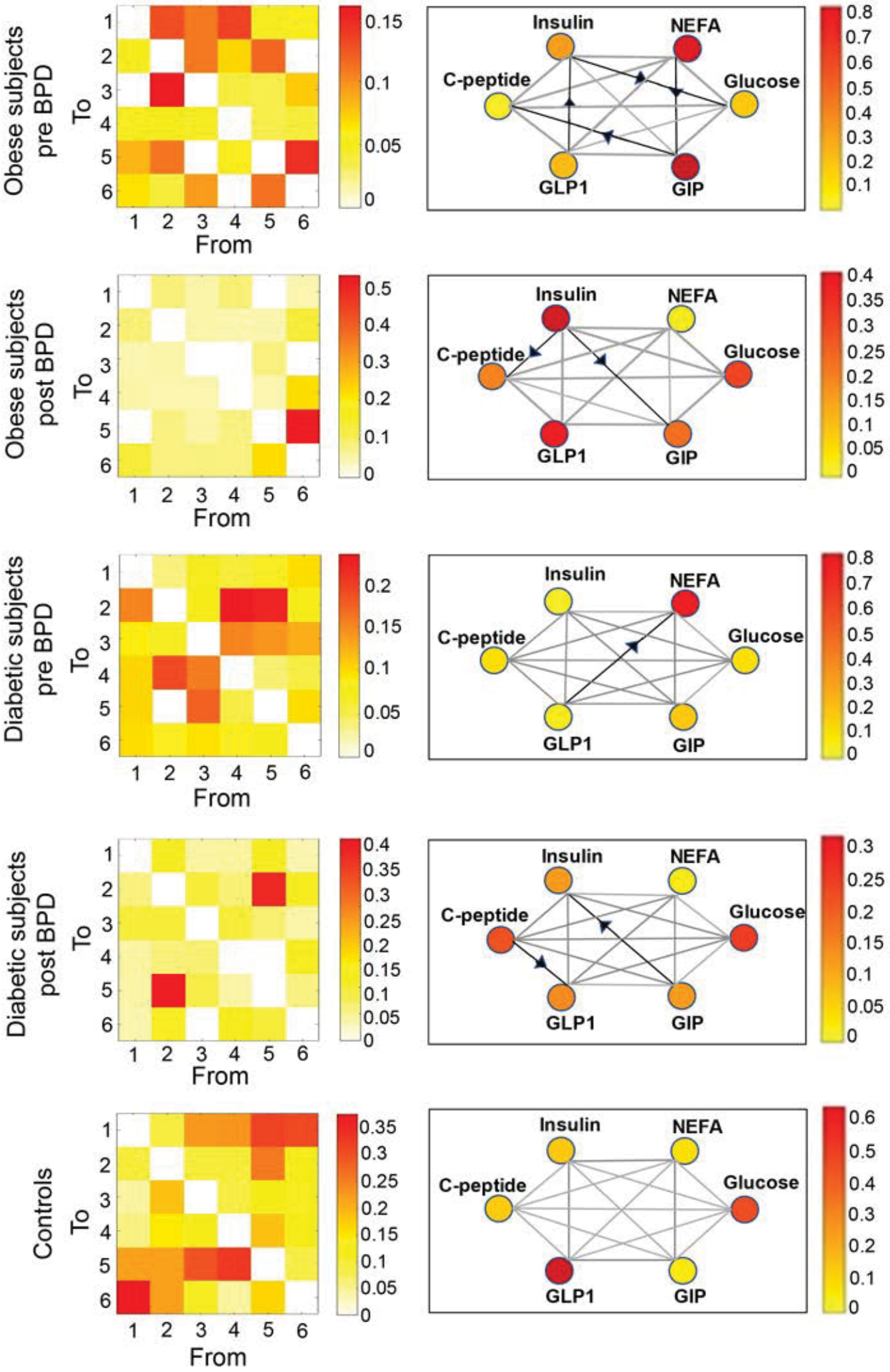
Obese subjects pre BPD
To
From
Insulin
NEFA
C-peptide
Glucose
GLP1
GIP
Obese subjects post BPD
Diabetic subjects pre BPD
Diabetic subjects post BPD
Controls